Histol Histopathol (2024) 39: 795-804

Histology and Histopathology
From Cell Biology to Tissue Engineering

ORIGINAL ARTICLE Open Access

Effects of sinomenine on a rat orthotopic liver carcinoma model

Yunlong Zhang[1], Hongmei Ran[1], Shanshan Hui[1] and Liping Qian[2]

[1]Department of Ultrasonography, Linping Campus, The Second Affiliated Hospital of Zhejiang University School of Medicine and [2]Department of Radiology, Hangzhou Cancer Hospital, Hangzhou, PR China

Summary. Objective. Liver carcinoma is a common malignant tumor. In this study, an orthotopic liver carcinoma model was established by B-ultrasound, and the therapeutic effect of sinomenine (Sin) on the disease was investigated.

Methods. SD rats were randomly divided into control, Sin, Sorafenib (Sor), and combination (Sin+Sor) groups (n=8). An orthotopic liver carcinoma model was established by inoculating N1-S1 cells into the rat liver by B-ultrasound-guided, and tumor volume was monitored three times by B-ultrasound after inoculation. After drug treatment, the tumor tissues were stained with HE and TUNEL, and the levels of inflammatory cytokines, ALT and AST were detected by ELISA. The numbers of erythrocytes, leukocytes and platelets were detected. Immunohistochemistry and immunofluorescence were used to detect the expression of Ki-67, CD44, VEGF and CD31. The levels of cell cycle, apoptosis-related proteins were detected by western blot.

Results. B-ultrasound monitoring found that Sin reduced tumor volume. Moreover, Sin improved tissue lesions, and promoted cancer cell apoptosis. Sin decreased the levels of inflammatory cytokines, AST and ALT, and decreased the numbers of erythrocytes, leukocytes and platelets. Simultaneously, the expressions of Ki-67, CD44, VEGF and CD31 were decreased in the Sin group. Furthermore, Sin decreased the Bcl-2, Cyclin D1, CDK4, CDK6 and Survivin levels, but increased Bax, Cleaved-caspase3/pro-caspase3, P21 and P27 levels. More importantly, the combination of Sin and Sor treatment was more effective than treatment alone.

Conclusion. A rat orthotopic liver carcinoma model was established under the guidance of B-ultrasound, and Sin had a therapeutic effect on orthotopic liver carcinoma.

Corresponding Author: Liping Qian, Department of Radiology, Hangzhou Cancer Hospital, Hangzhou 310002, PR China. e-mail: Nolan761@163.com

www.hh.um.es. DOI: 10.14670/HH-18-683

Key words: B-ultrasound, Liver carcinoma, Orthotopic tumor, Sinomenine

Introduction

Liver carcinoma is one of the most common malignant tumors, and its clinical manifestations include liver pain, fatigue, weight loss and other symptoms (Yan et al., 2022). Morbidity and mortality are high, and it imposes a serious burden on society and individuals (Su et al., 2022). Studies have found that surgical tumor resection and liver transplantation are the main treatment methods at present, but these two methods have problems such as high recurrence probability, difficult operation, lack of liver source, and poor prognosis (Leoni et al., 2022; Lu et al., 2022). Therefore, it is urgent and necessary to find potential therapeutic drugs for liver cancer.

B-ultrasound is the use of ultrasonic reflection, refraction and other physical properties in human tissue. Signals are received by the instrument to display the morphology of various tissues and organs to judge the lesion location, nature and degree of functional damage. The technology is used in clinical medicine for early diagnosis (Mueller et al., 2018; Hu et al., 2020; Rovida et al., 2022). There are various animal models of liver cancer, and intrahepatic injection of tumor cells through open abdomen is a common method for establishing orthotopic models of liver cancer (Jin et al., 2014). Cell injection guided by imaging technology, such as ultrasound equipment, greatly reduces the trauma and stress response of rats under the premise of ensuring the tumor formation rate (Buijs et al., 2012).

Sinomenine (Sin) is an alkaloid compound derived from the roots and stems of the ivy tree vine (Zheng et al., 2021). It has a variety of pharmacological activities such as sedative, anti-inflammatory, antibacterial, hypotensive, and immune regulation (Song et al., 2021). Recent studies have shown that Sin also has good anti-tumor effects, mainly by inhibiting tumor cell proliferation, inhibiting tumor invasion and metastasis, and inducing tumor cell

autophagy (Shen et al., 2020; Yang et al., 2021). Sin has also been reported to protect against alcohol-induced liver injury in model mice (Fan et al., 2022). However, there are few reports about Sin on liver carcinoma, so it is very important to explore whether Sin has a protective effect on orthotopic liver carcinoma.

In this study, a rat model of orthotopic liver carcinoma was established by injecting liver carcinoma cells under the guidance of ultrasound. Moreover, the growth of the tumor and the tumor-inhibitory effect of Sin was evaluated by means of ultrasonic imaging detection to explore the therapeutic effect of Sin on orthotopic liver carcinoma.

Materials and methods

Establishment of orthotopic liver carcinoma model and drug intervention

SD rats (6 w, 180-220 g) were obtained from the Centre of Experimental Animals at the Shanghai Jihui Laboratory Animal Care Co., Ltd (Certificate No. SCXK (Hu) 2017-0012; Shanghai, China), and housed in an environment with 23-25°C and humidity of 55-70%. SD rats were fed with a standard diet and allowed free access to water. The rats were divided into 4 groups (n=8): Control (Con), Sin, Sor (sorafenib) and Sin+Sor group. Anesthesia was induced in a gas mixture of 95% oxygen and 5% isoflurane and maintained with 0.25-4% isoflurane via a nose cone. The rats were then placed in a supine position, the abdominal area was shaved and disinfected with betadine, and N1-S1 cells (2×10^6 cells/rat, CRL-1604, ATCC) were inoculated under the guidance of ultrasound (Buijs, Geschwind et al., 2012). From day 11, Sin 20 mg/kg/d, Sor 7.5 mg/kg/d, and Sin 20 mg/kg/d +Sor 7.5 mg/kg/d were intraperitoneally injected in the Sin, Sor and Sin+Sor group, for 10 consecutive days, respectively. The Con group was injected with an equal volume of normal saline for 10 consecutive days.

B-ultrasound imaging for tumor formation monitoring

Rats were depilated for skin preparation, and an appropriate amount of ultrasound couplant was smeared on the exposed skin. The ultrasound probe on the digital color ultrasonic diagnostic apparatus [G50, VINNO Technology (Suzhou) Co., Ltd., China] was placed on the exposed skin to observe the tumor size changes in the monitor. In addition, tumor growth was detected by B-ultrasound on days 5, 10 and 20 from cell inoculation, and the size of two perpendicular diameters of each tumor was measured by B-ultrasound and expressed as the mean diameter.

On the 21st day, the rats in each group were euthanized by CO_2, peripheral blood was collected from the tail vein, and then the liver tissue was collected and stored for subsequent experiments. The abdominal cavity was dissected, ascites was collected, and liver tumor tissues were collected.

HE staining

10% formalin solution was used for fixation of liver tumor tissues for 12h. Then they were dehydrated by gradient ethanol, embedded in paraffin and cut into 5 μm sections for HE staining. The changes of liver tumor tissue structure were observed under a microscope. According to the results of HE staining, it was divided into 5 grades, with a score of 0-4. It mainly evaluates the infiltrated range of cancer cells in the liver tissue, the state of cells in the non-infiltrated part, and the intercellular space. The lower the score, the larger the infiltration range of the liver tissue by cancer cells, the damage to the cells in the non-infiltrated part, and the larger the intercellular space (Yousef et al., 2023).

TUNEL staining

The apoptosis of rat liver tumor tissues was detected by TUNEL kit (G1501, Servicebio, China). The paraffin sections were sequentially put into a gradient concentration of xylene and alcohol solution for dewaxing and dehydration. Then, the sections were reacted with proteinase K working solution at 37°C for 20 min, washed, dripped with rupture solution (G1204, Servicebio, China). Then we added equilibration buffer, mixed with TDT enzyme, dUTP, and buffer in the TUNEL kit according to the number of slices and tissue size, and then incubated for 1h. After washing 3 times with PBS, the sections were immersed in a dye vat containing DAPI solution (G1012, Servicebio, China) and incubated for 10 min. After mounting the slides, the sections were observed with a fluorescence microscope (Eclipse C1, Nikon, Japan).

Immunohistochemistry

Liver tumor tissues were immersed in a 4% paraformaldehyde solution for fixation for 2h. Then they were embedded in paraffin and cut into 5 μm sections. The liver sections were deparaffinized with xylene, dehydrated with gradient ethanol, and washed twice with water. The sections were incubated in 0.1% H_2O_2 solution for 30 min and rinsed with phosphate buffered saline 3 times, then blocked with 3% BSA, and then the primary antibodies Ki-67 (AF0198, 1:100, Affinity), CD44 (ab205921, 1:100, Abcam) and VEGF (ab32152, 1:100, Abcam) were added and incubated at 4°C overnight. Then the secondary antibody horseradish peroxidase-conjugated antibody (HRP) (ab97080, 1:500, Abcam) was added and incubated for 20 min. It was counterstained with hematoxylin for 3 min. Then the slices were observed with an optical microscope.

ELISA

The levels of IL-2, IL-6, IL-10 and TNF-α in liver

tumor tissue homogenate, and the contents of ALT and AST in rat plasma were detected by relevant ELISA kits. The ELISA kits information is as follows: IL-2, IL-10 (PI577, PI525, Beyotime Biotech Inc), IL-6, TNF-α, ALT and AST (MM-0163M1, MM-0132M1, ml058648, ml059334, Shanghai Enzyme Linked Biotechnology Co., Ltd.), respectively.

Blood cell counts

The peripheral blood of rats was taken for counting erythrocytes, leukocytes and platelets by ADVIA 120 hematology system (Siemens Healthcare GmbH, Erlangen, Germany).

Immunofluorescence

Liver tumor tissues were placed in a 4% paraformaldehyde solution for fixation for 2h. 5 μm-thick sections were cut, then the slides were deparaffinized in xylene. Then we use gradient alcohol for dehydration and washed twice with distilled water. The section was blocked with 3% BSA. A rabbit primary antibody CD31 (AF0077, 1:100, Affinity) was added and incubated overnight. Then, a secondary antibody HRP, HRP-goat anti-rabbit IgG (ab97080, 1:500, Abcam) was added and incubated for 20 min. After that, peroxidase activity was induced and amplified with FITC-tyramide (B40932, 1:500, Thermo). Finally, the sections are stained with DAPI staining solution in the dark for 10 min. Then we added an autofluorescence quencher for 5 min, rinsed with water, mounted the slides, and observed and collected images by a fluorescence microscope.

Western blot

The levels of Bcl-2, Bax, Cleaved-caspase3, Pro-Caspase3, Cyclin D1, CDK4, CDK6, P21, P27 and Survivin in the rat liver tumor tissue were measured by western blot. First, we collected the total protein in rat liver tumor tissue and used the BCA protein kit (Solarbio, pc0020) to detect the total protein concentration. The tissue lysates were resolved in 10% or 12% SDS-PAGE gels and electrophoretically transferred onto a PVDF membrane. Then we blocked the PVDF membrane with 5% skimmed milk powder, put the membrane into the primary antibody Bcl-2 (AF6139, 1:1000, Affinity), Bax (AF0120, 1:2000, Affinity), Cleaved-caspase3 (AF7022, 1:1000, Affinity), Pro-Caspase3 (AF3311, 1:1000, Affinity), CyclinD1(AF0931, 1:1000, Affinity), CDK4 (DF6102, 1:1000, Affinity), CDK6 (DF6448, 1:1000, Affinity), P21 (AF6290, 1:1000, Affinity), P27 (AF6324, 1:1000, Affinity), Survivin (AF6017, 1:1000, Affinity) and β-actin (AF7018,1:10000, Affinity) and incubated it overnight. Then the membrane was rinsed and HRP incubated for 20 min. The protein bands were detected by the ECL and the protein gray value was calculated by Image J.

Statistical analysis

SPSS 19.0 was used for data analysis. One-way ANOVA analysis of variance was used to compare data differences among multiple groups, and *post hoc* Tukey test was used for comparison between groups. Shapiro-Wilk was used to test the normality of the data. All data were expressed as mean ± standard deviation. $P<0.05$ was regarded as statistically significant.

Results

Sin reduced tumor volume in rats

The ultrasound imaging results are shown in Figure 1. It can be seen that within 10 days after cell inoculation, there was no significant difference in the volume of liver tumors among the groups. After 20 days, relative to the Con group, the liver tumor volume of the rats in the Sin, Sor and the Sin+Sor group was significantly reduced. And Sin and Sor co-treatment suppressed tumor formation most notably.

The effect of Sin on histopathological changes of liver tumor

The results of HE staining are shown in Figure 2a. The liver tumor tissue of the rats in the Con group was massively infiltrated by tumor cells, forming a complete tumor structure. The liver tumor tissue in the Sin, Sor, and the Sin+Sor group was also infiltrated to varying degrees, but the infiltrated volume was much smaller than that in the control group. In addition, the HE semi-quantitative scores of liver tumor tissue in the Sin, Sor, and the Sin+Sor group were significantly higher than those in the Con group (Fig. 2b). The infiltrated liver tumor tissue in the Sin+Sor group was smaller than that in the Sin and Sor groups, but the semi-quantitative scores were higher than that in the Sin and Sor groups.

Sin promoted apoptosis in rat liver tumor tissue

The results of Sin on apoptosis of rat liver tumor cells are shown in Figure 2c. The apoptosis rates of rat liver tumor cells in the Sin, Sor, and the Sin+Sor group were significantly higher than that in the Con group (Fig. 2d). Furthermore, the Sin+Sor group had the highest apoptosis rate of liver tumor cells.

Effects of Sin on the levels of inflammatory cytokines in rat liver tumor tissue and the contents of ALT and AST in rat plasma

The results in Figure 3 show that the levels of IL-2, IL-6 and TNF-α in the liver tumor tissue of the Sin, Sor, and Sin+Sor group were significantly lower than those of the Con group, while the level of IL-10 did not change significantly. Moreover, the levels of ALT and

AST in the plasma of the rats in the Sin, Sor, and Sin+Sor group were significantly lower than those in the Con group. The improvement of inflammatory factors and ALT and AST levels in the Sin+Sor group was better than that in the Sin group and Sor group.

Sin reduced the number of erythrocytes, leukocytes and platelets in rat plasma

The effect of Sin on the number of erythrocytes, leukocytes and platelets in the plasma of rats observed by light microscope is shown in Figure 4. It could be observed that the numbers of erythrocytes, leukocytes and platelets in the plasma of the Sin, Sor, and Sin+Sor group were lower than those of the Con group. Moreover, the numbers of erythrocytes, leukocytes and platelets in the plasma of Sin+Sor group were lower than those of Sin group and Sor group.

Sin reduced the expression levels of Ki-67, CD44 and VEGF in liver tumor tissues of rats

The immunohistochemical results are shown in Figure 5. The expression levels of Ki-67, CD44 and VEGF in liver tumor tissues of rats in the Sin, Sor, and Sin+Sor group were lower than those in the c Con group.

Sin reduced the expression levels of CD31 in liver tumor tissues of rats

The immunofluorescence results are shown in Figure 6. The protein expression of CD31 in the liver tumor tissue of the Sin, Sor, and Sin+Sor was significantly lower than that of the Con group. The combined effect of

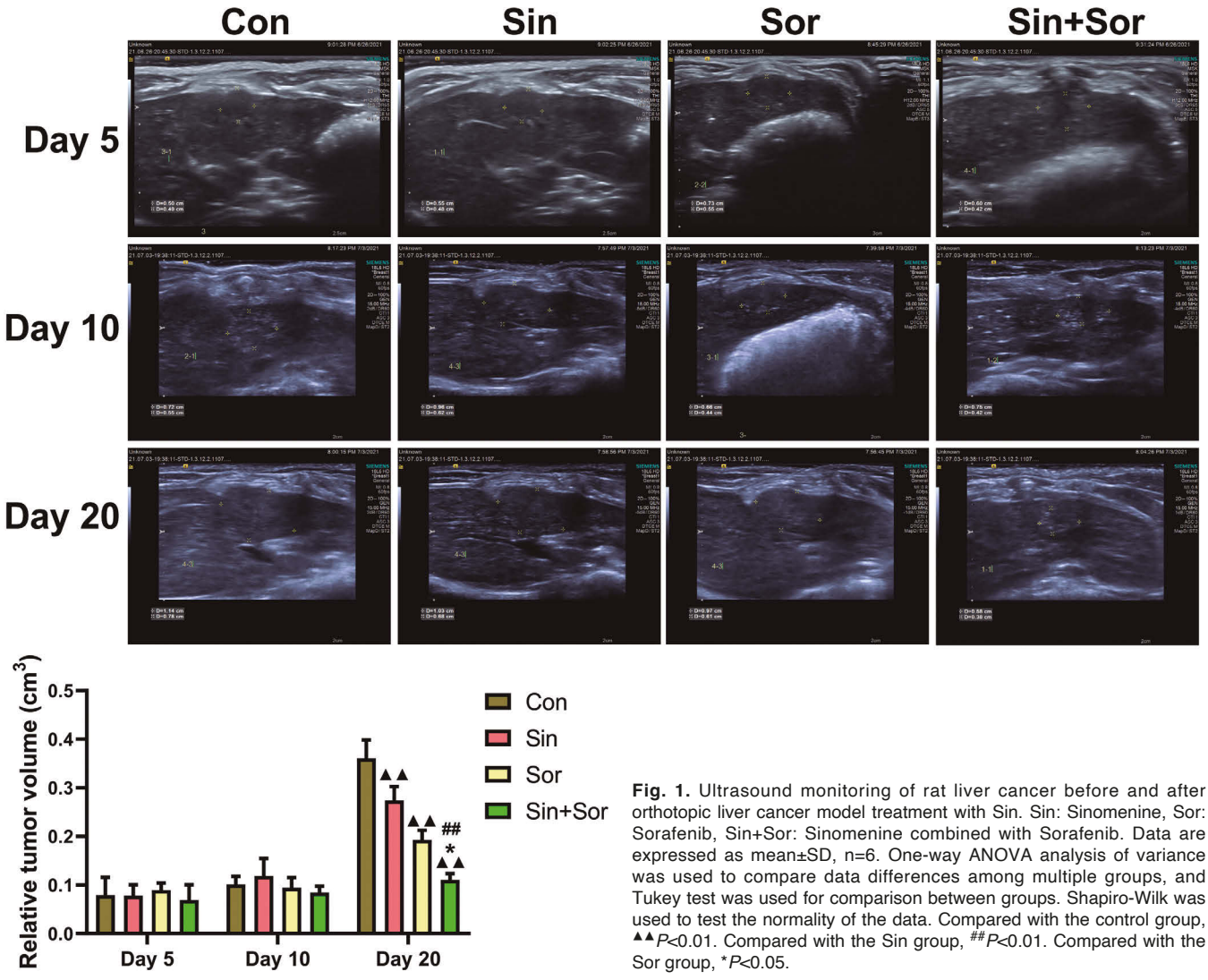

Fig. 1. Ultrasound monitoring of rat liver cancer before and after orthotopic liver cancer model treatment with Sin. Sin: Sinomenine, Sor: Sorafenib, Sin+Sor: Sinomenine combined with Sorafenib. Data are expressed as mean±SD, n=6. One-way ANOVA analysis of variance was used to compare data differences among multiple groups, and Tukey test was used for comparison between groups. Shapiro-Wilk was used to test the normality of the data. Compared with the control group, ▲▲P<0.01. Compared with the Sin group, ##P<0.01. Compared with the Sor group, *P<0.05.

Sin+Sor was better than that of Sin and Sor alone.

Effects of Sin on the expressions of cell apoptosis and the cycle-related proteins in rat liver tumor tissues

The western blot results are shown in Figure 7. The levels of Bax, Cleaved-caspase 3/Pro-caspase 3, P21 and P27 proteins in the rat liver tumor tissue of the Sin, Sor, and Sin+Sor group were higher than those of the Con group, while the levels of Bcl-2, Cyclin D1, CDK4, CDK6 and Survivin were lower than those in the Con group. The effect of Sin+Sor group on cell apoptosis and cycle-related proteins is better than that of Sin, Sor group.

Discussion

Liver carcinoma is one of the malignant tumors that seriously threaten human health (Tang et al., 2018). Research on new treatment methods and drugs for liver cancer has always been a hot spot in clinical and basic research (Dawkins and Webster, 2019), and rat animal models also play an indispensable role in liver carcinoma research. Ultrasound-guided injection inoculation is one of the transplantation methods to establish orthotopic liver cancer models with few traumas for experimental animals. What's more, the orthotopic liver cancer model established by B-ultrasound has a higher tumor formation rate and faster growth rate, and ultrasound can monitor the growth of tumors *in vivo*, which has certain advantages (Chan et al., 2010). In this study, we established a rat orthotopic liver cancer model under the guidance of B-ultrasound, and then found that the volume of the *in situ* tumor was significantly higher on the 20th day of modeling than on the 5th and 10th day.

Sin is an alkaloid with antitumor effects on various cancers (Cao et al., 2021; Song et al., 2022). Studies

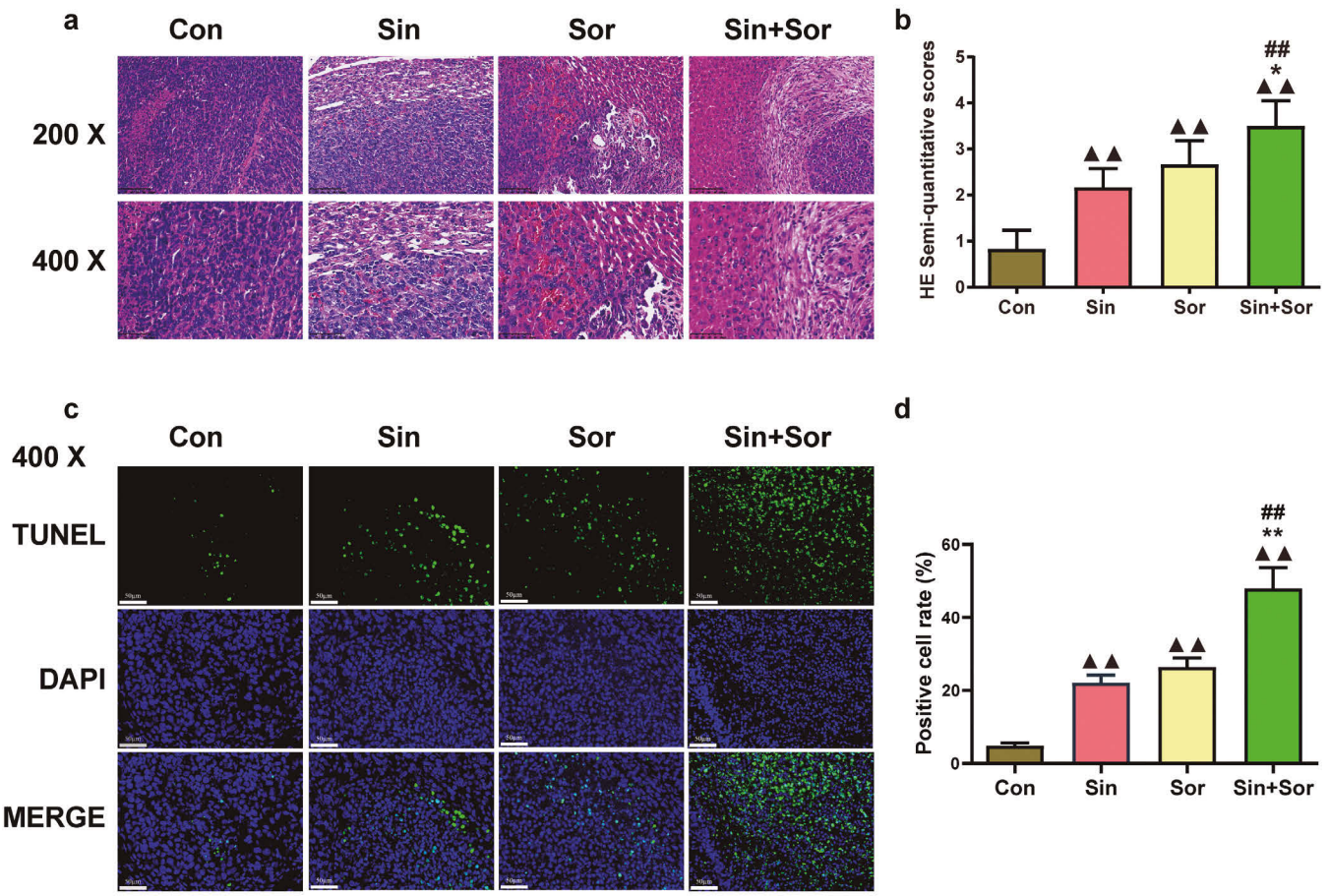

Fig. 2. Effects of Sin on histopathological changes and apoptosis of rat liver tumors. **a.** HE staining on the pathological changes of rat liver tumor tissue. **b.** Tunel staining on the apoptosis of rat liver tumor tissue cells. Data are expressed as mean±SD, n=6. One-way ANOVA analysis of variance was used to compare data differences among multiple groups, and Tukey test was used for comparison between groups. Shapiro-Wilk was used to test the normality of the data. Compared with the control group, ▲▲P<0.01. Compared with the Sin group, ##P<0.01. Compared with the Sor group, *P<0.05, **P<0.01. Sin: Sinomenine, Sor: Sorafenib, Sin+Sor: Sinomenine combined with Sorafenib.

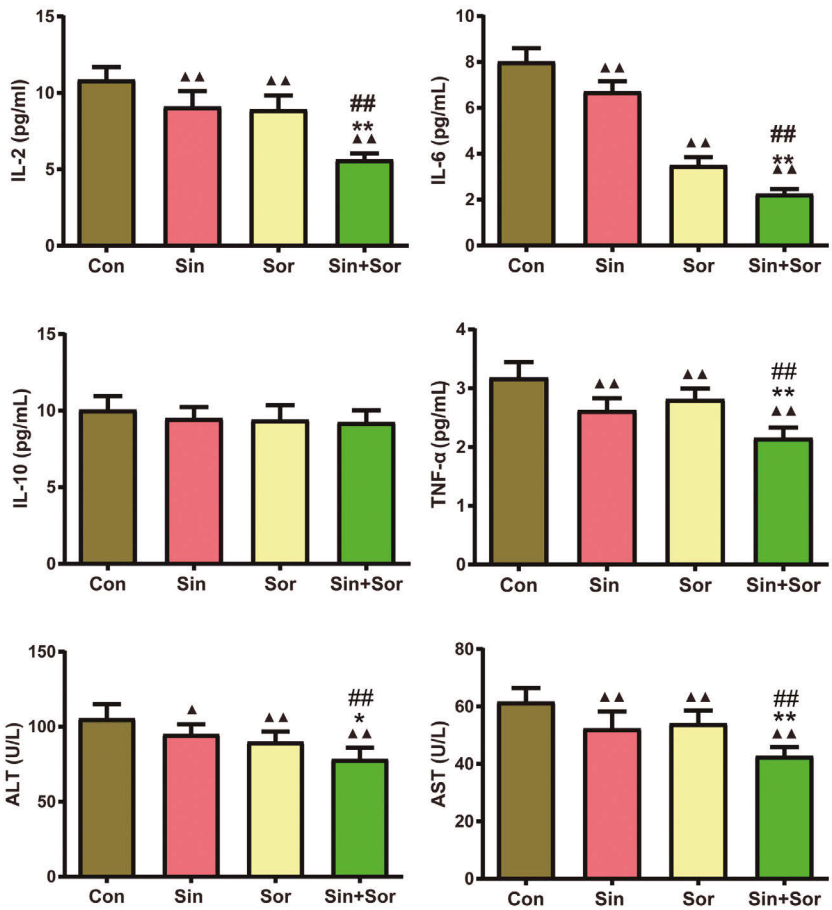

Fig. 3. The effect of Sin on the levels of IL-2, IL-6, IL-10, TNF-α in rat liver tumor tissue and the contents of ALT and AST in rat plasma. Sin: Sinomenine, Sor: Sorafenib, Sin+Sor: Sinomenine combined with Sorafenib. Data are expressed as mean±SD, n=8. One-way ANOVA analysis of variance was used to compare data differences among multiple groups, and Tukey test was used for comparison between groups. Shapiro-Wilk was used to test the normality of the data. Compared with the control group, $^{\blacktriangle}P<0.05$, $^{\blacktriangle\blacktriangle}P<0.01$. Compared with the Sin group, $^{\#\#}P<0.01$. Compared with the Sor group, $^{*}P<0.05$, $^{**}P<0.01$.

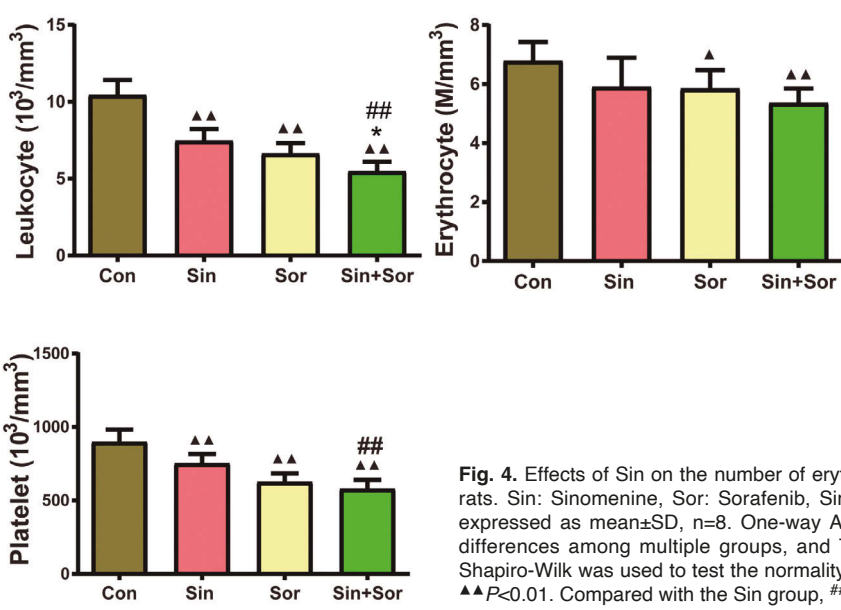

Fig. 4. Effects of Sin on the number of erythrocytes, leukocytes and platelets in peripheral blood of rats. Sin: Sinomenine, Sor: Sorafenib, Sin+Sor: Sinomenine combined with Sorafenib. Data are expressed as mean±SD, n=8. One-way ANOVA analysis of variance was used to compare data differences among multiple groups, and Tukey test was used for comparison between groups. Shapiro-Wilk was used to test the normality of the data. Compared with the control group, $^{\blacktriangle}P<0.05$, $^{\blacktriangle\blacktriangle}P<0.01$. Compared with the Sin group, $^{\#\#}P<0.01$. Compared with the Sor group, $^{*}P<0.05$.

have found that Sin can alleviate alcohol-induced liver injury and promote liver injury cell apoptosis (Lu et al., 2013; Chen et al., 2020). This is similar to the result that Sin can alleviate the pathological damage of rat liver tumor tissue and promote the apoptosis of liver tumor tissue in this study. Previous studies have shown that Sin can regulate the levels of IL-6, IL-12, IL-10 and TNF-α in rheumatoid arthritis mice and dry eye mice (Liu et al., 2018; Li et al., 2020). Furthermore, Sin can also reduce the levels of ALT and AST in the serum of mice with liver injury (Chen et al., 2020). Our study showed that Sin decreased IL-2, IL-6 and TNF-α levels in rat liver tumor tissue and ALT and AST levels in rat plasma. This further illustrates that Sin can reduce inflammatory factors and AST/ALT levels, to suppress the inflammatory environment and alleviate liver injury, thus inhibiting liver carcinoma progression. Moreover, Sin combined with Sor reduced the levels of IL-2, IL-6 and TNF-α in rat liver tumor tissue and the levels of ALT and AST in rat plasma better than Sin or Sor alone. This indicated that Sin addition has a synergetic effect on Sor for tumor inhibition.

The development of hepatocellular carcinoma *in situ* activates the body's inflammatory and immune responses, resulting in increased white blood cell counts. He et al found that platelets promoted the proliferation of hepatocellular carcinoma cells (He et al., 2017). In previous years, erythroid-associated parameters have been indicated to be linked to liver-associated diseases (Hu et al., 2013; Wei et al., 2016). A previous study has reported that the erythrocyte count in peripheral blood was associated with survival after surgery in patients with primary liver cancer (Xie et al., 2015). In this study, the numbers of erythrocytes, leukocytes and platelets were highly expressed in the peripheral blood of rats, and the levels of erythrocytes, leukocytes and platelets were reversed after Sin treatment. In addition, Sin combined with Sor was found to be more effective in reducing erythrocytes, leukocytes and platelets than Sin or Sor administered alone in this study.

The expression of Ki-67 has been recognized as a good indicator of tumor proliferation (Abdel-Hamid et

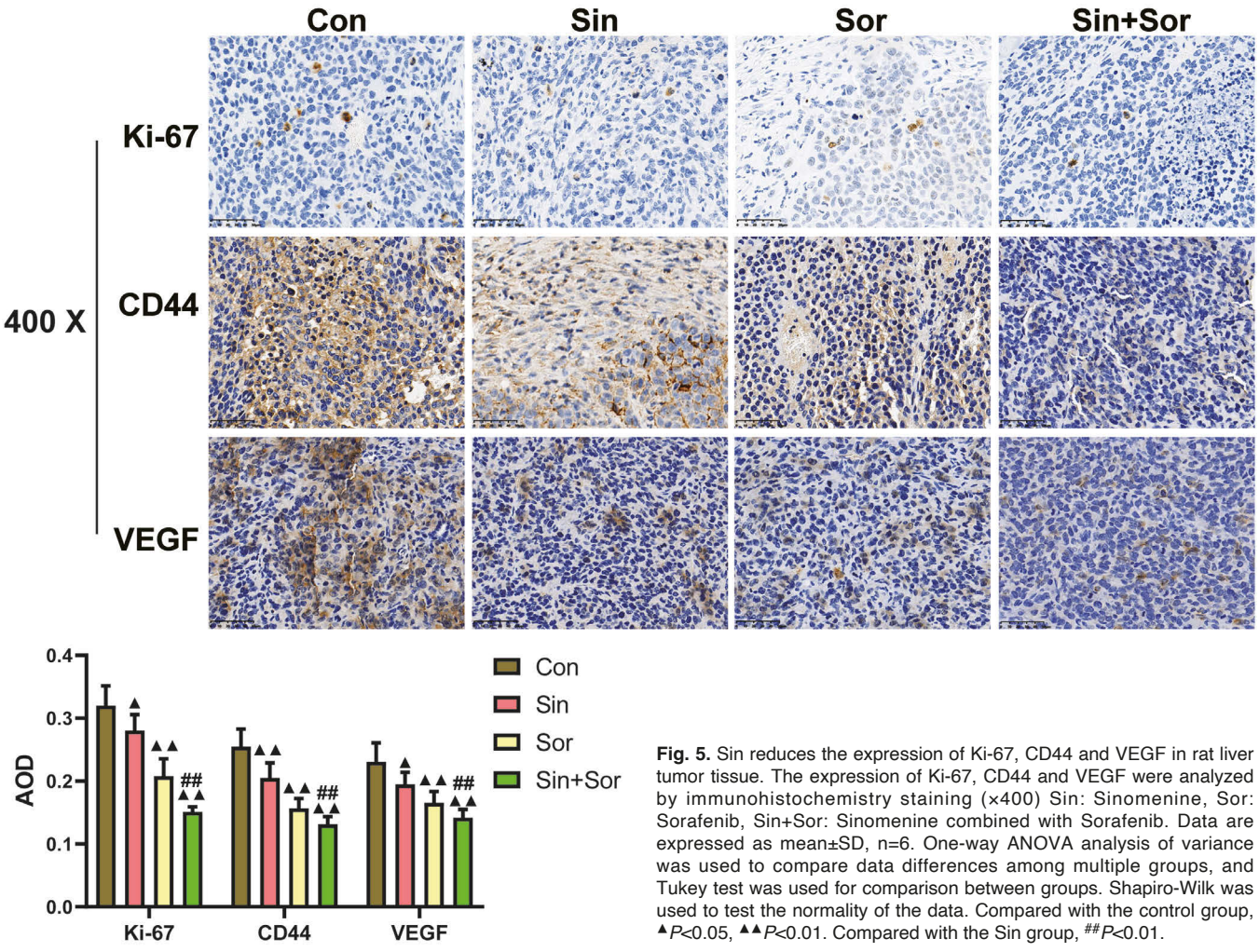

Fig. 5. Sin reduces the expression of Ki-67, CD44 and VEGF in rat liver tumor tissue. The expression of Ki-67, CD44 and VEGF were analyzed by immunohistochemistry staining (×400) Sin: Sinomenine, Sor: Sorafenib, Sin+Sor: Sinomenine combined with Sorafenib. Data are expressed as mean±SD, n=6. One-way ANOVA analysis of variance was used to compare data differences among multiple groups, and Tukey test was used for comparison between groups. Shapiro-Wilk was used to test the normality of the data. Compared with the control group, $^{▲}P<0.05$, $^{▲▲}P<0.01$. Compared with the Sin group, $^{\#\#}P<0.01$.

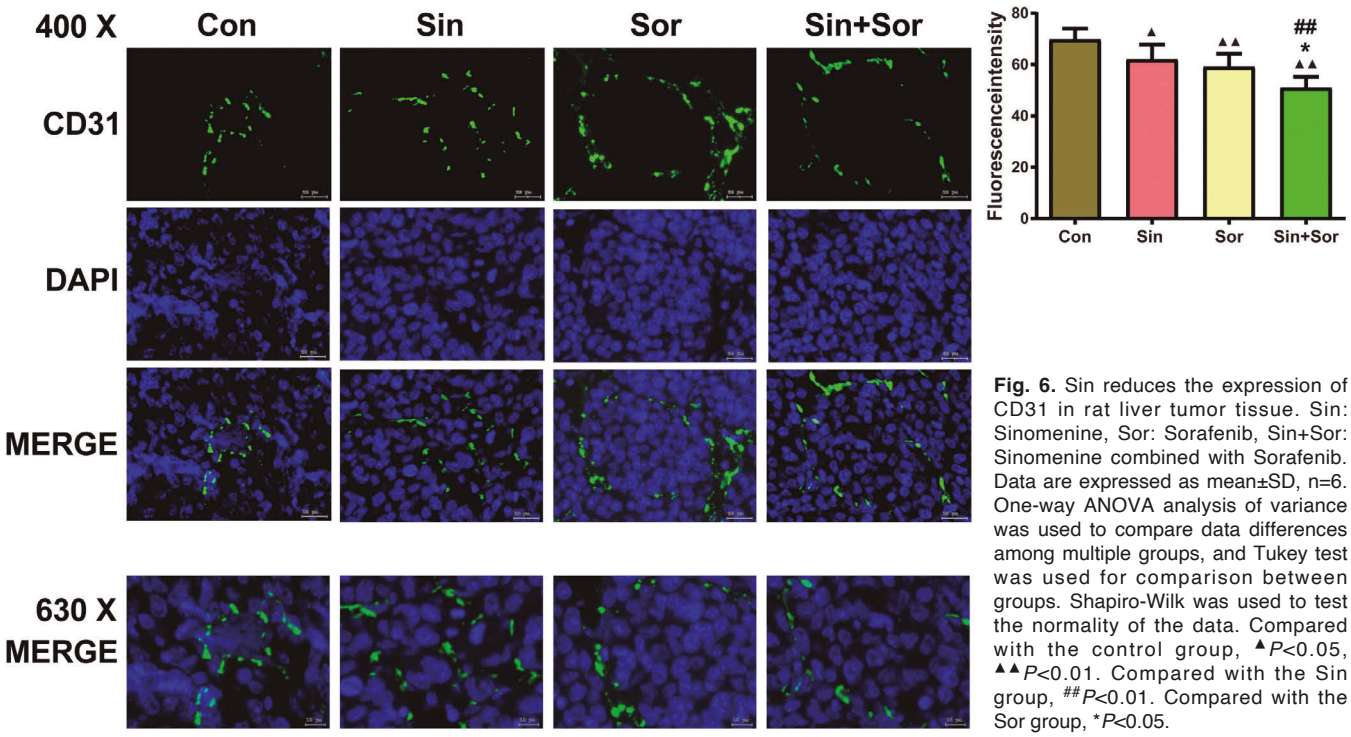

Fig. 6. Sin reduces the expression of CD31 in rat liver tumor tissue. Sin: Sinomenine, Sor: Sorafenib, Sin+Sor: Sinomenine combined with Sorafenib. Data are expressed as mean±SD, n=6. One-way ANOVA analysis of variance was used to compare data differences among multiple groups, and Tukey test was used for comparison between groups. Shapiro-Wilk was used to test the normality of the data. Compared with the control group, $^{\blacktriangle}P<0.05$, $^{\blacktriangle\blacktriangle}P<0.01$. Compared with the Sin group, $^{\#\#}P<0.01$. Compared with the Sor group, $^{*}P<0.05$.

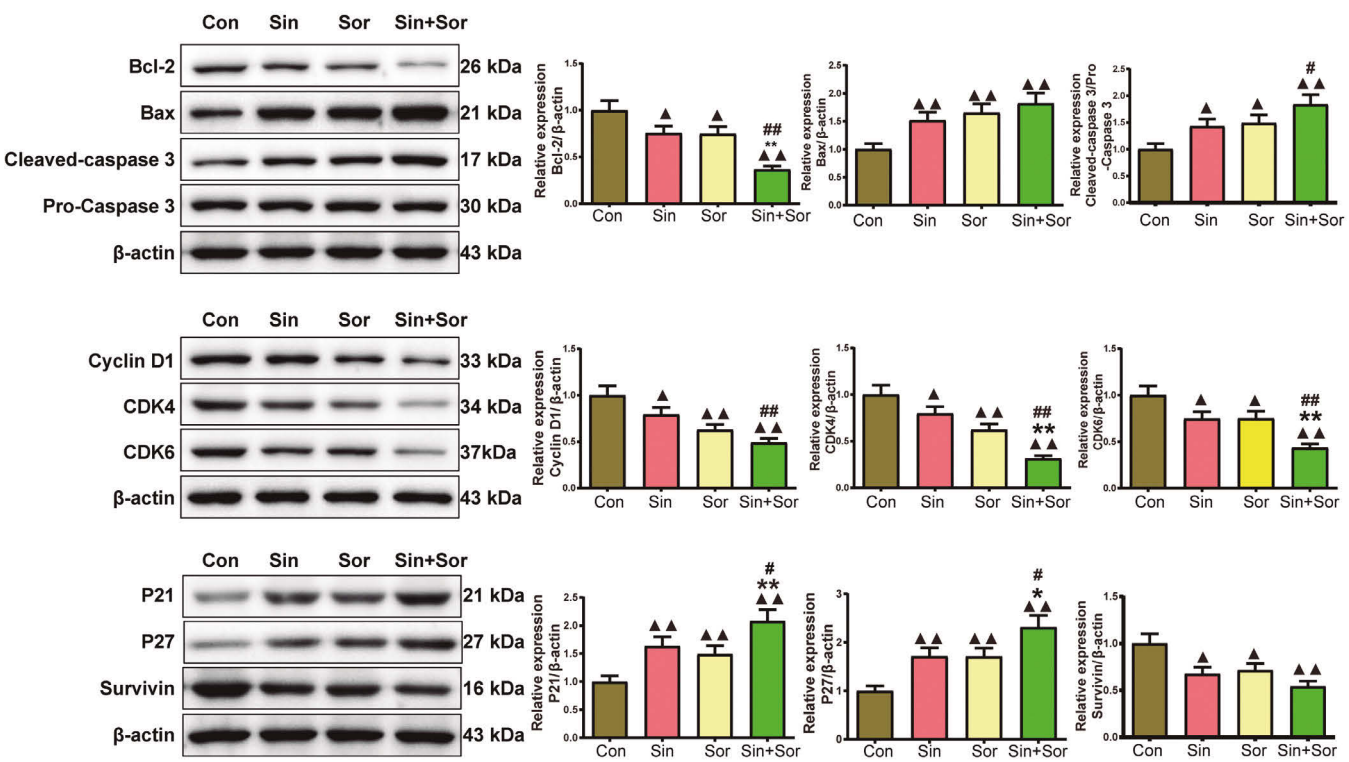

Fig. 7. Effects of Sin on the expression of Bcl-2, Bax, Cleaved-caspase3/pro-caspase3, Cyclin D1, CDK4, CDK6, P21, P27 and Survivin proteins in rat liver tumor tissue. Sin: Sinomenine, Sor: Sorafenib, Sin+Sor: Sinomenine combined with Sorafenib. Data are expressed as mean±SD, n=3. One-way ANOVA analysis of variance was used to compare data differences among multiple groups, and Tukey test was used for comparison between groups. Shapiro-Wilk was used to test the normality of the data. Compared with the control group, $^{\blacktriangle}P<0.05$, $^{\blacktriangle\blacktriangle}P<0.01$. Compared with the Sin group, $^{\#}P<0.05$, $^{\#\#}P<0.01$. Compared with the Sor group, $^{*}P<0.05$, $^{**}P<0.01$.

al., 2022). CD44 plays a role in the invasion and metastasis of tumor cells (Tan et al., 2022). In addition, Kato et al found that overexpression of Ki-67, CD44 and VEGF all promoted tumorigenesis (Kato et al., 2020). In this study, Ki-67, CD44, and VEGF were highly expressed in liver tumor tissues, and the levels of Ki-67, CD44, and VEGF were reversed after Sin treatment. Similar studies found that Sin reduced Ki-67 expression in esophageal cancer and VEGF expression in arthritic mice (Fu et al., 2018; Feng et al., 2019). Furthermore, we found that Sin could reduce the expression of CyclinD1, Bcl-2, CDK4, CDK6 and Survivin and increase the expression of Bax, Cleaved-caspase-3/pro-caspase-3, P21 and P27 in rat liver tumor tissue. This is similar to the results of previous studies on the effect of Sin on apoptosis, cycle and the expression of new apoptosis-related proteins in tumor tissues (Wang et al., 2018, 2021). In addition, in this study Sin combined with Sor in rats with hepatocellular carcinoma *in situ* the treatment effect was better.

This study mainly discussed the establishment of rat orthotopic liver carcinoma under the guidance of B-ultrasound, and the research on the resistance of Sin to liver carcinoma. However, this study also has certain limitations. The mechanism of action of Sin on liver carcinoma has not yet been stated clearly and needs to be further explored.

In conclusion, this study established a rat orthotopic liver carcinoma under the guidance of B-ultrasound based on previous work and demonstrated the therapeutic effect of Sin on liver carcinoma, which provides a theoretical and experimental basis for the treatment of liver carcinoma.

Acknowledgements. None.

Conflict of interest statement. There is no conflict of interest between the authors of this article.

Ethics approval and consent to participate. This study was approved by Animal Experimentation Ethics Committee of Hangzhou Eyong Biotechnological Co., Ltd. Animal Experiment Center (approval no. ZJEY-20210923-07).

References

Abdel-Hamid N.M., Zakaria S., Nawaya R.A., Eldomany R.A. and El-Shishtawy M.M. (2022). Daidzein and chicory extract arrest the cell cycle via inhibition of cyclin D/CDK4 and cyclin A/CDK2 gene expression in hepatocellular carcinoma. Recent Pat. Anticancer Drug Discov. 18, 187-199.

Buijs M., Geschwind J.F., Syed L.H., Ganapathy-Kanniappan S., Kunjithapatham R., Wijlemans J.W., Kook Kwak B., Ota S. and Vali M. (2012). Spontaneous tumor regression in a syngeneic rat model of liver cancer: implications for survival studies. J. Vasc. Interv. Radiol. 23, 1685-1691.

Cao J., Huang J., Gui S. and Chu X. (2021). Preparation, synergism, and biocompatibility of *in situ* liquid crystals loaded with sinomenine and 5-Fluorouracil for treatment of liver cancer. Int. J. Nanomedicine 16, 3725-3739.

Chan H.H., Chu T.H., Chien H.F., Sun C.K., Wang E.M., Pan H.B., Kuo H.M., Hu T.H., Lai K.H., Cheng J.T. and Tai M.H. (2010). Rapid induction of orthotopic hepatocellular carcinoma in immune-competent rats by non-invasive ultrasound-guided cells implantation. BMC Gastroenterol. 10, 83.

Chen H., Wang Y., Jiao F.Z., Yang F., Li X. and Wang L.W. (2020). Sinomenine attenuates acetaminophen-induced acute liver injury by decreasing oxidative stress and inflammatory response via regulating TGF-β/Smad pathway *in vitro* and *in vivo*. Drug Des. Devel. Ther. 14, 2393-2403.

Dawkins J. and Webster R.M. (2019). The hepatocellular carcinoma market. Nat. Rev. Drug Discov. 18, 13-14.

Fan H., Tu T., Zhang X., Yang Q., Liu G., Zhang T., Bao Y., Lu Y., Dong Z., Dong J. and Zhao P. (2022). Sinomenine attenuates alcohol-induced acute liver injury via inhibiting oxidative stress, inflammation and apoptosis in mice. Food Chem. Toxicol. 159, 112759.

Feng Z.T., Yang T., Hou X.Q., Wu H.Y., Feng J.T., Ou B.J., Cai S.J., Li J. and Mei Z.G. (2019). Sinomenine mitigates collagen-induced arthritis mice by inhibiting angiogenesis. Biomed. Pharmacother. 113, 108759.

Fu S., Jin L., Gong T., Pan S., Zheng S., Zhang X., Yang T., Sun Y., Wang Y., Guo J., Hui B. and Zhang X. (2018). Effect of sinomenine hydrochloride on radiosensitivity of esophageal squamous cell carcinoma cells. Oncol. Rep. 39, 1601-1608.

He A.D., Xie W., Song W., Ma Y.Y., Liu G., Liang M.L., Da X.W., Yao G.Q., Zhang B.X., Gao C.J., Xiang J.Z. and Ming Z.Y. (2017). Platelet releasates promote the proliferation of hepatocellular carcinoma cells by suppressing the expression of KLF6. Sci. Rep. 7, 3989.

Hu Z., Sun Y., Wang Q., Han Z., Huang Y., Liu X., Ding C., Hu C., Qin Q. and Deng A. (2013). Red blood cell distribution width is a potential prognostic index for liver disease. Clin. Chem. Lab. Med. 51, 1403-1408.

Hu L., Zhao J.S., Xing C., Xue X.L., Sun X.L., Dang R.F., Chen W.Z., Wang Z.B. and Chen J.Y. (2020). Comparison of focused ultrasound surgery and hysteroscopic resection for treatment of submucosal uterine fibroids (FIGO type 2). Ultrasound Med. Biol. 46, 1677-1685.

Jin Y., Tong D., Shen J., Yang J. and Li J. (2014). Establishment of experimental implantation tumor models of hepatocellular carcinoma in Wistar rats. Tumor Biol. 35, 9079-9083.

Kato H., Naiki-Ito A., Yamada T., Suzuki S., Yamashita Y., Inaguma S., Kondo N., Wanifuchi-Endo Y., Toyama T. and Takahashi S. (2020). The standard form of CD44 as a marker for invasion of encapsulated papillary carcinoma of the breast. Pathol. Int. 70, 835-843.

Leoni J., Rougemont A.L., Calinescu A.M., Ansari M., Compagnon P., Wilde J.C.H. and Wildhaber B.E. (2022). Effect of centralization on surgical outcome of children operated for liver tumors in Switzerland: A retrospective comparative study. Children (Basel), 9, 217.

Li H., Wei F., Li S., Yan L. and Lu P. (2020). The effect of sinomenine eye drops on experimental dry eye in mice. Cutan. Ocul. Toxicol. 39, 389-395.

Liu W., Zhang Y., Zhu W., Ma C., Ruan J., Long H. and Wang Y. (2018). Sinomenine inhibits the progression of rheumatoid arthritis by regulating the secretion of inflammatory cytokines and monocyte/macrophage subsets. Front. Immunol. 9, 2228.

Lu X.L., Zeng J., Chen Y.L., He P.M., Wen M.X., Ren M.D., Hu Y.N., Lu G.F. and He S. (2013). Sinomenine hydrochloride inhibits human hepatocellular carcinoma cell growth *in vitro* and *in vivo*: involvement

of cell cycle arrest and apoptosis induction. Int. J. Oncol. 42, 229-238.

Lu R.Y., Zhu H.K., Liu X.Y., Zhuang L., Wang Z.Y., Lei Y.L., Wang T. and Zheng S.S. (2022). A Non-Linear relationship between preoperative total bilirubin level and postoperative delirium incidence after liver transplantation. J. Pers. Med. 12, 141.

Mueller R., Grunke M., Wendler J., Schuch F., Hofmann-Preiss K., Boettger I., Jakobs R., Schulze-Koops H. and Von Kempis J. (2018). The value of an automated ultrasound system in the detection of synovitis. Ultrasound Int. Open 4, E61-e68.

Rovida S., Orso D., Naeem S., Vetrugno L. and Volpicelli G. (2022). Lung ultrasound in blunt chest trauma: A clinical review. Ultrasound 30, 72-79.

Shen K.H., Hung J.H., Liao Y.C., Tsai S.T., Wu M.J. and Chen P.S. (2020). Sinomenine Inhibits Migration and Invasion of Human Lung Cancer Cell through Downregulating Expression of miR-21 and MMPs. Int. J. Mol. Sci. 21, 3080.

Song W., Yang X., Wang W., Wang Z., Wu J. and Huang F. (2021). Sinomenine ameliorates septic acute lung injury in mice by modulating gut homeostasis via aryl hydrocarbon receptor/Nrf2 pathway. Eur. J. Pharmacol. 912, 174581.

Song L., Tang L., Lu D., Hu M., Liu C., Zhang H., Zhao Y., Liu D. and Zhang S. (2022). Sinomenine inhibits vasculogenic mimicry and migration of breast cancer side population cells via regulating miR-340-5p/SIAH2 axis. BioMed Res. Int., 2022, 4914005.

Su G.F., Huang Z.X., Huang D.L., Chen P.X., Wang Y. and Wang Y.F. (2022). Cepharanthine hydrochloride inhibits the Wnt/β-catenin/Hedgehog signaling axis in liver cancer. Oncol. Rep. 47, 83.

Tan L.Y., Cockshell M.P., Moore E., Myo Min K.K., Ortiz M., Johan M.Z., Ebert B., Ruszkiewicz A., Brown M.P., Ebert L.M. and Bonder C.S. (2022). Vasculogenic mimicry structures in melanoma support the recruitment of monocytes. Oncoimmunology 11, 2043673.

Tang A., Hallouch O., Chernyak V., Kamaya A. and Sirlin C.B. (2018). Epidemiology of hepatocellular carcinoma: target population for surveillance and diagnosis. Abdom. Radiol. (NY), 43, 13-25.

Wang Y., Li M., Yu X., Chen A., Ding Y., Wang Y. and Wang Y. (2018). Sinomenine hydrochloride inhibits cell survival in human hepatoma Huh7 cells. Biomed. Rep. 8, 510-516.

Wang Y., Zhao L., Yuan W., Liang L., Li M., Yu X. and Wang Y. (2021). A natural membrane vesicle exosome-based sinomenine delivery platform for hepatic carcinoma therapy. Curr. Top. Med. Chem. 21, 1224-1234.

Wei T.T., Tang Q.Q., Qin B.D., Ma N., Wang L.L., Zhou L. and Zhong R.Q. (2016). Elevated red blood cell distribution width is associated with liver function tests in patients with primary hepatocellular carcinoma. Clin. Hemorheol. Microcirc. 64, 149-155.

Xie X., Yao M., Chen X., Lu W., Lv Q., Wang K., Zhang L. and Lu F. (2015). Reduced red blood cell count predicts poor survival after surgery in patients with primary liver cancer. Medicine (Baltimore) 94, e577.

Yan Z., Lijuan Y., Yinhang W., Yin J., Jiamin X., Wei W., Yuefen P. and Shuwen H. (2022). Screening and analysis of RNAs associated with activated memory CD4 and CD8 T cells in liver cancer. World J. Surg. Oncol. 20, 2.

Yang W., Feng Q., Li M., Su J., Wang P., Wang X., Yin Y., Wang X. and Zhao M. (2021). Sinomenine suppresses development of hepatocellular carcinoma cells via inhibiting MARCH1 and AMPK/STAT3 signaling pathway. Front. Mol. Biosci. 8, 684262.

Yousef E.H., Abo El-Magd N.F. and El Gayar A.M. (2023). Carvacrol enhances anti-tumor activity and mitigates cardiotoxicity of sorafenib in thioacetamide-induced hepatocellular carcinoma model through inhibiting TRPM7. Life Sci. 324, 121735.

Zheng X., Li W., Xu H., Liu J., Ren L., Yang Y., Li S., Wang J., Ji T. and Du G. (2021). Sinomenine ester derivative inhibits glioblastoma by inducing mitochondria-dependent apoptosis and autophagy by PI3K/AKT/mTOR and AMPK/mTOR pathway. Acta Pharm. Sin. B 11, 3465-3480.

Accepted November 30, 2023